

Photorefractive holograms recorded in a variable field perpendicular to the lattice vector: theory and experiment

Yu. V. Miklyaev and V. I. Safonov

Chelyabinsk State Technical University, 454080 Chelyabinsk, Russia

(Submitted 20 March 1995)

Zh. Éksp. Teor. Fiz. **110**, 95–104 (July 1996)

Recording of holograms in a photorefractive crystal by light beams whose frequency difference equals the frequency of an external ac electric field is studied in the case in which this field is directed parallel to the fringes of the interference pattern. © 1996 American Institute of Physics. [S1063-7761(96)00807-4]

1. INTRODUCTION

The nature of the photorefractive effect and its application to recording, preserving, and processing information¹ is actively being studied at present. There are several methods of recording holograms in photorefractive crystals in which one uses an external (dc or ac) electric field.^{1,2} As a rule, the direction of this field is chosen parallel to the wave vector of the intensity grating \mathbf{q} (i.e., perpendicular to the fringes of the interference pattern). One of the methods of recording that uses an external field is synchronous detection.^{3,4} This mechanism produces grating if the recording is effected with beams of different frequencies, while the frequency of the external ac field equals the difference of the frequencies of the recording beams and is far smaller than the reciprocal of the time for recording the hologram.

References 5 and 6 discussed the possibility of using this mechanism in the case in which the field is directed perpendicular to the grating vector \mathbf{q} . Reference 5 proposed and studied theoretically the recording of holograms in a plane photorefractive waveguide with an ac field applied perpendicular to the surfaces of the waveguide. This recording geometry allows one to attain in the crystal considerably higher intensities of the applied field than when one records in a bulk crystal or in a waveguide with the external field parallel to the grating vector. In the present case the maximum voltage between the electrodes will no longer be limited by surface breakdown, but by bulk breakdown. The small distance between the electrodes also enables one to obtain high electric field intensities inside the photorefractive medium at low voltages between the electrodes. Reference 6 experimentally realized recording of holograms in a bulk crystal by beams of different frequencies in the case in which the ac external field was perpendicular to the grating vector \mathbf{q} . The signal wave and the pump wave were focused by a cylindrical lens. This recording method can be considered to model a plane photorefractive waveguide. The present study theoretically and experimentally examines the mechanism of recording holograms with this interaction geometry.

A diagram of the interaction is shown in Fig. 1. The pump wave and the signal wave, focused by a cylindrical lens, create an interference pattern in the photorefractive crystal. One applies an external ac electric field of frequency Ω to the crystal parallel to the interference fringes. As in the case of synchronous detection discussed earlier,^{3,4} the fre-

quency difference Ω between the waves creating the interference pattern equals the frequency of the external field.

Let us study the interaction mechanism of the waves in the photorefractive crystal qualitatively (Fig. 2). We assume that the external field varies as $E_0(t) = E_0 \text{sign}[\cos(\omega t)]$, while instead of a traveling interference pattern one uses an interference pattern that shifts jumpwise by half the period $\Lambda = 2\pi/q$ when the direction of the external field changes. The external field leads to drift of electrons from the illuminated regions of the photorefractive crystal into the unilluminated regions. The concentration of electrons in the conduction band at the maxima of the interference pattern is greater than at the minima. Therefore the electrons will be concentrated opposite the maxima of the interference pattern in the first half of the period of the external field in regions corresponding to negative y coordinates (Fig. 2a). In the second half of the period the direction of the external field is reversed, and the maxima and minima of the interference pattern exchange places. As a result the negative charges will be concentrated opposite the maxima of the new interference pattern (shifted by $\Lambda/2$) in the regions corresponding to positive y coordinates (Fig. 2b). Thus, during the course of a large number of periods of the external field, a grating created by the field of the space charge is recorded in the crystal.

2. THEORY

For theoretical analysis of the recording mechanism, we use a well-known model of grating formation in a photorefractive crystal.⁷ According to this model, the process is described by a system of equations consisting of the kinetic equation, Ohm's law, the equation of continuity, and Poisson's equation:

$$\frac{\partial N^+}{\partial t} = s(I + \beta_I)(N_D - N^+) - \gamma n N^+, \quad (1)$$

$$\mathbf{j} = e\mu n \mathbf{E} + kT\mu \nabla n, \quad (2)$$

$$\frac{\partial n}{\partial t} = \frac{\partial N^+}{\partial t} + \frac{1}{e} \text{div } \mathbf{j}, \quad (3)$$

$$\text{div } \mathbf{E} = -e(n + N_A - N^+)/\epsilon\epsilon_0. \quad (4)$$

Here n , N_A , N^+ , and N_D are the concentrations of electrons, acceptors, ionized and unionized donors, respectively; I is

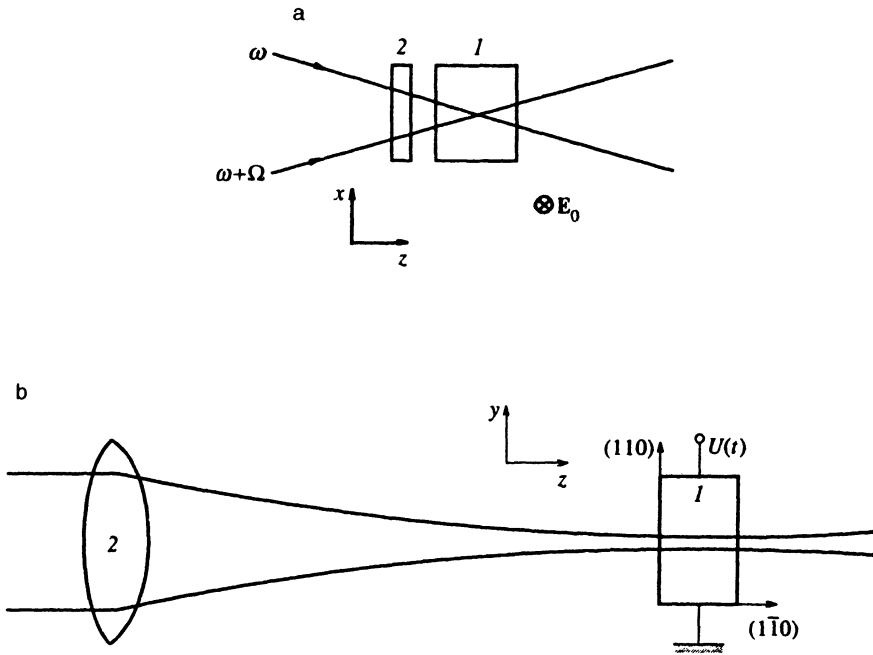


FIG. 1. Diagram of the two-wave interaction: a) the pump wave with frequency ω and the signal wave with frequency $\omega+\Omega$ illuminate a photorefractive crystal (1); b) the waves are focused by the cylindrical lens (2). An external ac field perpendicular to the grating vector is applied to the crystal.

the light intensity; s and γ are the photoionization and recombination constants; \mathbf{E} is the electric field; $e>0$ is the charge of the electron; \mathbf{j} is the electric current density; k_B is Boltzmann's constant; T is the temperature; β_t is the thermal ionization coefficient, μ is the electron mobility; and ϵ and ϵ_0 are the dielectric constants of the medium and the vacuum.

Using the usual condition for a photorefractive medium $n \ll N_A \ll N_D$ and neglecting the diffusion current $k_B T \mu \nabla n$ in

comparison with the drift current $e \mu n \mathbf{E}$, we transform the system of equations (1)–(4) to the form

$$\frac{sN_D}{\gamma N_A} (I + \beta_t) - n - \frac{n \epsilon \epsilon_0}{e N_A} \operatorname{div} \mathbf{E} + \frac{\mu}{\gamma N_A} \operatorname{div}(n \mathbf{E}) = 0, \quad (5)$$

$$\tau_M \frac{\partial \operatorname{div} \mathbf{E}}{\partial t} = -\operatorname{div}(n \mathbf{E}). \quad (6)$$

Here $\tau_M = \epsilon \epsilon_0 / \sigma$ is the Maxwell relaxation time, and σ is the conductivity of the crystal.

In the interaction geometry being studied, the radiation intensity $I(x, y, t)$ and the electric field have the form

$$I(x, y, t) = I_0(y) \left[1 + \frac{m(t)}{2} \exp(iqx) + \text{c.c.} \right], \quad (7)$$

$$\mathbf{E}(x, y, t) = \mathbf{E}_0 \operatorname{sign}[\cos(\Omega t)] + \mathbf{E}_{sc}(x, y, t), \quad (8)$$

where Ω is the frequency of the external field, $\mathbf{E}_0 = (E_{0x}, E_{0y})$ is its amplitude, \mathbf{E}_{sc} is the field of the space charge, $m(t) = |m| \exp(i\Omega t)$ is the contrast of the interference pattern, and q is the spatial frequency of the grating.

Certain properties of the field distribution of the space charge can be derived from the symmetry of the interaction without solving the system of equations (5)–(8). Let us consider separately the cases in which the direction of the external field is perpendicular and parallel to the lattice vector.

In the former case, if the transverse distribution of the light intensity $I_0(y)$ is symmetric, then the potential of the field of the space charge $\phi(y)$ ($E_{scx} = -\partial\phi/\partial x$, $E_{scy} = -\partial\phi/\partial y$) is antisymmetric. Consequently the x component of the field $E_{scx}(y)$ is an antisymmetric function, while the y component $E_{scy}(y)$ is symmetric. The diffraction efficiency of the hologram is proportional to the square of the overlap integral of the intensities of the waves and the modulation of the refractive index due to the interaction:

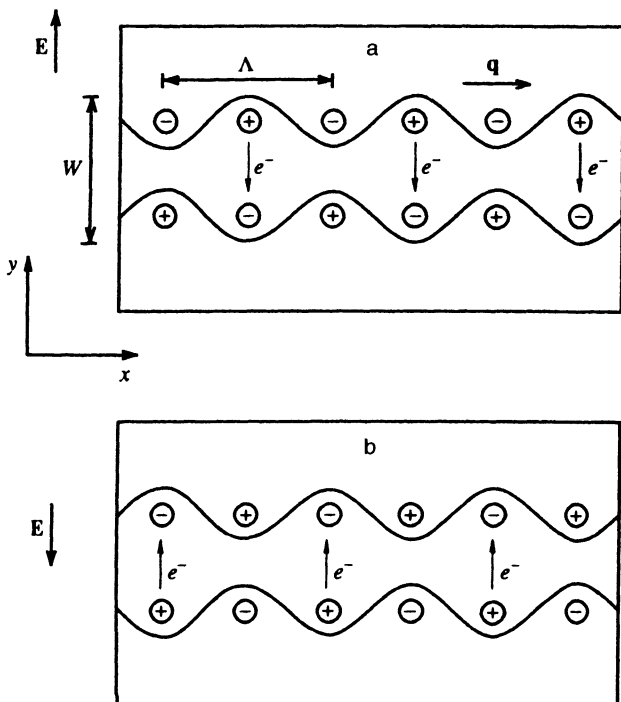


FIG. 2. Transverse cross section of the photorefractive crystal for the first (a) and second (b) halves of the period of the external field.

$$\int E_{sc}(y)I_0(y)dy.$$

This integral vanishes for the x component of the field:

$$\int E_{scx}(y)I_0(y)dy=0.$$

Therefore it is necessary that the y component of the field of the space charge produce the modulation of the refractive index, which is achieved by choosing the polarization of the incident light and/or the orientation of the crystal.

Yet if the external field is parallel to the grating vector and the transverse profile of the light intensity $I_0(y)$ is symmetric, the potential of the field of the space charge $\varphi(y)$ is also symmetric. Consequently the overlap integral vanishes for the y component of the field of the space charge:

$$\int E_{scy}(y)I_0(y)dy=0.$$

Therefore in recording the hologram it is necessary that the x component of the field produce the modulation of the refractive index.

We solve Eqs. (5)–(8) for the special case in which the drift length of an electron $l_E=E_{0y}\mu/\gamma N_A$ and the Debye screening radius $l_q=E_{0y}\epsilon\epsilon_0/eN_A$ are much smaller than either the period of the interference pattern $\Lambda=2\pi/q$ or the dimensions of the Gaussian beam waist W . These conditions are satisfied by the $\text{Bi}_{12}\text{TiO}_{20}$ crystal used in the experiment. We perform the following calculations for a small contrast ($m \ll 1$) of the interference pattern. Upon taking account of the assumptions that we have made and averaging over the period of the external field, we transform Eqs. (5)–(8) into a differential equation:

$$\begin{aligned} & -\tau_M \frac{\partial}{\partial t} \left(\frac{\partial^2 \varphi}{\partial y^2} - q^2 \varphi \right) \\ & = (I_0 + \beta) \left(\frac{\partial^2 \varphi}{\partial y^2} - q^2 \varphi \right) + \frac{\partial I_0}{\partial y} \frac{\partial \varphi}{\partial y} - \langle m(t) E_{0y}(t) \rangle \frac{\partial I_0}{\partial y} \\ & \quad - iq \langle m(t) E_{0x}(t) \rangle I_0. \end{aligned} \quad (9)$$

Here $\langle \dots \rangle$ denotes averaging over the period of the external field.

Equation (9) was numerically integrated for an intensity distribution $I(y)=\exp(y^2/4W^2)$ and a value of the parameter $\beta_l/I_0(0)=0.0001$.

The diffraction efficiency of the hologram η is

$$\sqrt{\eta} = \frac{1}{2} n^3 r_{\text{eff}} \frac{\pi d}{\lambda} \frac{\int E_{cs}(y)I_0(y)dy}{\int I_0(y)dy}, \quad (10)$$

where n is the refractive index of the crystal, λ is the wavelength of the light, d is the length of the crystal in the direction of propagation of the light, and r_{eff} is the effective electrooptic coefficient.

Figure 3 shows the theoretical relationship of the diffraction efficiency η to the spatial frequency q of the hologram for an external field parallel to the grating vector ($E_{0x}=E_0$, $E_{0y}=0$), and perpendicular to the grating vector ($E_{0x}=0$,

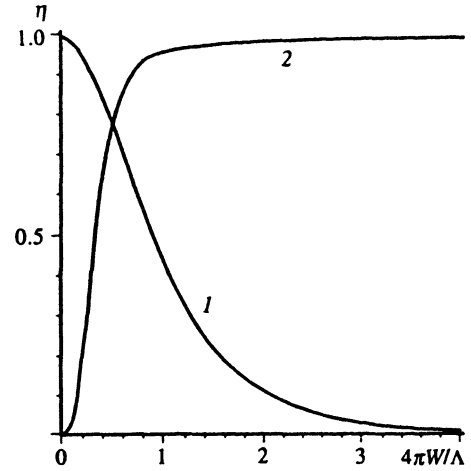


FIG. 3. Dependence of the diffraction efficiency η on the spatial frequency q of the grating for an external field perpendicular to the grating vector, $\mathbf{E}_0 \perp \mathbf{q}$ (curve 1) and parallel to the grating vector, $\mathbf{E}_0 \parallel \mathbf{q}$ (curve 2). The graphs are normalized to the value of the diffraction efficiency as $q \rightarrow 0$ when the holograms are recorded with a field perpendicular to the grating vector. The calculations used the following values of the parameters: $l_E/\Lambda = l_q/\Lambda = 0$, $\beta_l/I_0(0) = 0.0001$.

$E_{0y}=E_0$). Both graphs are normalized to the value of the diffraction efficiency as $q \rightarrow 0$ for holograms with a field perpendicular to the grating vector.

As we see from the relationships that have been given, recording holograms by using a perpendicular grating vector of the field is effective only if the beam waist W is much smaller than the period Λ of the interference pattern. In the case of a field parallel to the grating vector, the diffraction efficiency of the hologram η_{\parallel} equals zero for $q=0$, and rapidly reaches its maximum with increasing spatial frequency of the grating q . This value coincides with the diffraction efficiency of a hologram $\eta_{\perp}(0)$ in the case of a field perpendicular to the grating vector as $q \rightarrow 0$. As is known,⁸ when one records a grating without focusing the radiation with an ac field parallel to the grating vector, the diffraction efficiency of the hologram η does not depend on the spatial frequency of the grating if the drift length of an electron l_E and the screening radius l_q are much smaller than the grating period Λ . In the latter case the diffraction efficiency equals the quantity $\eta_{\parallel}(q)$ obtained in the case of focusing the radiation for large spatial frequencies q .

3. EXPERIMENT AND DISCUSSION

In this experiment we determined the dependence of the diffraction efficiency of holograms formed by the method described above on the spatial frequency q of the grating. The experimental setup is shown in Fig. 4. The radiation of a He-Ne laser was divided with a beamsplitter into signal and reference beams. The frequency of the reference beam was shifted by using a piezomirror to which a sawtooth voltage was applied. The ac voltage $E_0(t) = E_0 \text{sign}[\cos(\Omega t)]$ with frequency 33 Hz and amplitude 3.4 kV was applied to the (110) faces of the crystal. The distance between the electrodes was 7.6 mm, and the thickness of the crystal in the

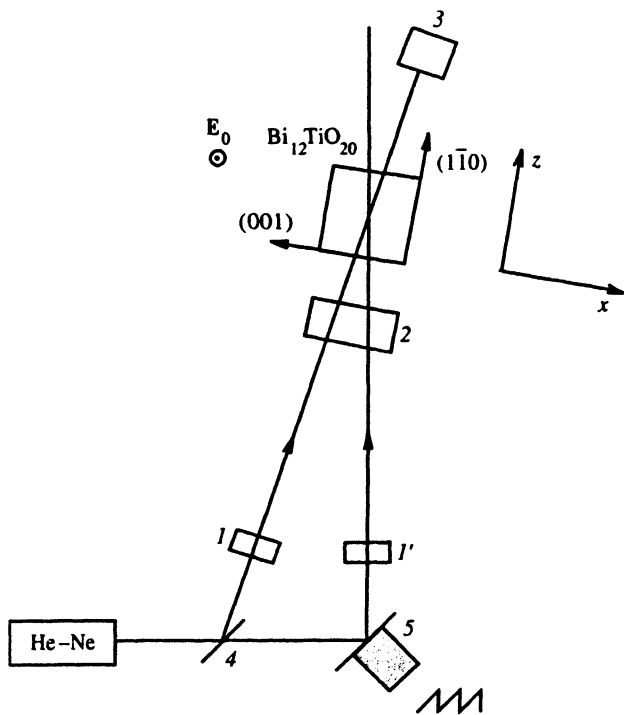


FIG. 4. Experimental setup: 1 and 1'—polarizers, 2—cylindrical lens, 3—photodiode, 4—beamsplitter, 5—piezomirror.

direction of propagation of light (along the $(1\bar{1}0)$ axis) was 5.5 mm. The wave vector of the grating was directed along the (001) axis.

The formation of a beam waist in the crystal of a size comparable to the period of the grating was achieved by focusing the radiation along the y axis (see Fig. 1) by using a cylindrical lens. In this experiment the lenses had focal lengths of 11.5 cm and 4.5 cm. The diameter of the beams in the plane of the lens was 3.5 mm, which made possible beam waist dimensions of $W=22 \mu\text{m}$ and $9 \mu\text{m}$, respectively.

The intensity of the signal wave following the crystal was measured with a photodetector. The diffraction efficiency was determined from the initial portion of the curve of erasure of the hologram as the ratio

$$\eta = \frac{I_D}{I_P} = \frac{I_D}{I_S} \beta, \quad (11)$$

where I_D is the intensity of the diffracted light, I_S and I_P are the intensities of the signal and reference beams, and β is the ratio of the intensities of the signal and reference beams, which was fixed at $\beta=I_S/I_P=10^{-2}$.

The choice of polarization was determined by the orientation of the crystal and its optical activity, $r=6 \text{ deg/mm}$. In order that the polarization direction at the center of the beam waist (in the middle of the crystal) coincide with the direction of the axis of the optical indicatrix of the crystal, which was deformed by the external field, the angle between the plane of polarization and the plane of incidence was set at 30° at the incident face of the crystal.

Figure 5 shows the dependence of the diffraction efficiency of the hologram η on the spatial frequency q for a field perpendicular to the grating vector. This diagram shows the theoretical dependences as solid lines, and the experimental data as dots. The experiments used lenses of focal lengths 11.5 cm (Fig. 5a) and 4.5 cm (Fig. 5b).

The best agreement between the theoretical and experimental data was obtained for an effective electrooptic coefficient $r_{\text{eff}}=6.7 \times 10^{-12} \text{ m/V}$. This value of the electrooptic coefficient is somewhat larger than that given in the literature for crystals of $\text{Bi}_2\text{TiO}_{20}$, $r_{\text{eff}}=5.8 \times 10^{-12} \text{ m/V}$.¹ We can explain the discrepancy as follows. In the theoretical treatment, for the sake of simplicity, the influence of the x component of the space charge field E_{scx} was not taken into account. However, with the orientation of the crystal used in the experiment, the x component of the field of the space charge also contributed to the change in the refractive index. The grating formed by this component of the field of the space charge led to diffraction of the TEM_{00} wave into the TEM_{01} wave. This factor then led to an increase in the diffraction efficiency.

In recording a lattice in a bulk crystal without focusing the radiation, in the case in which the external field is parallel to the grating vector, in the range of spatial frequencies $q=0.5 \times 10^3 - 4 \times 10^3 \text{ cm}^{-1}$ that we employed in the experiments discussed above, the diffraction efficiency did not de-

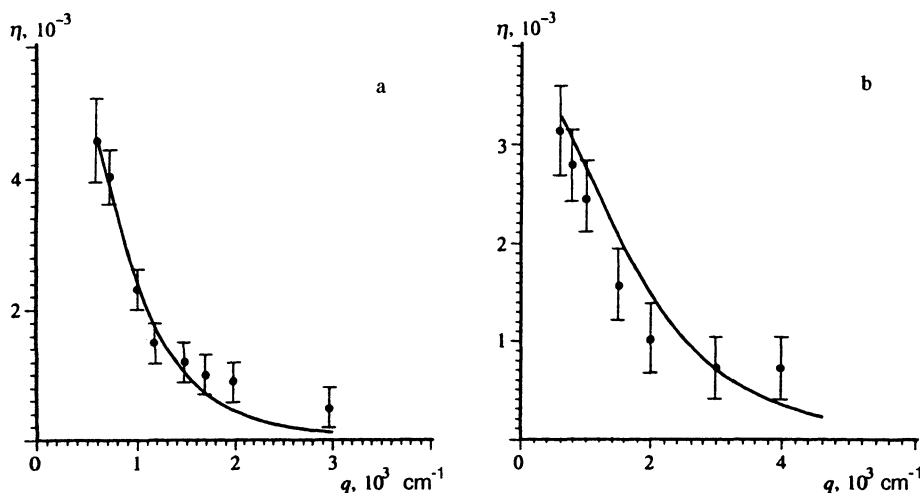


FIG. 5. Theoretical (curve) and experimental (dots) dependence of the diffraction efficiency η on the spatial frequency q of the grating for an external field perpendicular to the grating vector. The graphs were obtained for a Gaussian beam waist $W=22 \mu\text{m}$ (a) and $W=9 \mu\text{m}$ (b).

pend on the magnitude of q . This confirms the assumption made earlier of the smallness of the drift length l_E of an electron and the screening length l_q in comparison with the grating period Λ ,⁸ and indicates that the form of the spatial-frequency characteristics $\eta(q)$ shown in Fig. 5 is characteristic specifically of recording gratings with a field perpendicular to the wave vector. The value of the effective electrooptic coefficient $r_{\text{eff}}=4.8 \times 10^{-12}$ m/V in experiments without focusing the radiation was found to be somewhat lower than in experiments on recording holograms using an ac field perpendicular to the grating vector. The differences can also be explained by the influence of the x component of the field of the space charge upon focusing the radiation, which was not taken into account in the theoretical model.

Note that it was not possible to record a nonzero grating of the refractive index if the external field perpendicular to the wave vector is dc, and the interference pattern created by the waves focused by the cylindrical lens is stationary. This is explained by the fact that when one applies a dc field to a nonuniformly illuminated crystal, the field will be screened in the illuminated region. Perhaps recording in this geometry can be achieved when the dark conductivity is at least of the order of the photoconductivity.

Let us study the possible applications of the recording geometry investigated in this paper. The recording of holograms in a planar waveguide in which the external field was perpendicular to the surfaces of the waveguide was discussed in Ref. 5. In this case one can easily ensure conditions for efficient recording of the hologram ($W < \Lambda$) when the wave vector q of the grating lies in the plane of the waveguide.

In recording holograms with a speckle field, a situation can arise in which the fringes of the interference pattern have different orientations in different regions of the crystal. The wave vector q of the lattice in different regions of the crystal is directed arbitrarily, and one cannot fix a direction of the external field parallel to the vector q over the entire hologram. Recording of regions of the hologram where the interference fringes are parallel to the external field can be effected by the variant described in this study of the mechanism of synchronous detection if the dimensions of the speckle spots are comparable to the period of the interference

pattern. The recording of the regions of the hologram in which the interference fringes are perpendicular to the field will occur here also by the mechanism of synchronous detection described in Refs. 3 and 4. Therefore, in a hologram having a complex spatial structure all its regions will be recorded approximately uniformly. It was noted above that when one applies a dc field perpendicular to the wave vector of the grating, recording of a hologram does not occur. This leads us to believe that the mechanism of synchronous detection in recording such holograms can prove highly preferable. As we see it, this problem demands further study.

4. CONCLUSION

This study has demonstrated the possibility of recording holograms with an external field perpendicular to the wave vector q of the grating. The mechanism of recording is efficient if the grating period exceeds the dimensions of the illuminated region in the direction of the external field. The theoretical calculations performed on the basis of the known model of formation of gratings in a photorefractive crystal⁷ agree with the experimental data.

This study was supported by the International Science Fund (Grant MMM 000).

The authors thank B. Ya. Zel'dovich and N. D. Kundikova for valuable discussions, and V. G. Trofimov for aid in organizing the experiment.

¹M. P. Petrov, S. I. Stepanov, and A. V. Khomenko, *Photosensitive Electrooptic Media in Holography and Optical Image Processing* (in Russian), Nauka, Leningrad (1983).

²*Photorefractive Materials and Their Applications*, Vol. 1, P. Gunter and J.-P. Huignard (eds.), Springer-Verlag, Berlin-Heidelberg (1988).

³B. Ya. Zel'dovich, P. N. Il'inykh, and O. P. Nesterkin, *Zh. Éksp. Teor. Fiz.* **98**, 861 (1990) [*Sov. Phys. JETP* **71**, 478 (1990)].

⁴B. Ya. Zel'dovich, P. N. Il'inykh, and O. P. Nesterkin, *Pis'ma Zh. Tekh. Fiz.* **15** 20, 78 (1989) [*Sov. Tech. Phys. Lett.* **15**, 820 (1989)].

⁵Yu. V. Miklyaev, V. I. Safonov, and B. Ya. Zel'dovich, *Opt. Commun.* **113**, 476 (1995).

⁶Yu. V. Miklyaev, *JETP Lett.* **60**, 524 (1994).

⁷N. V. Kukhtarev, V. B. Markov, S. G. Odulov *et al.*, *Ferroelectrics* **22**, 949 (1979).

⁸A. V. Dooghin, B. Ya. Zel'dovich, P. N. Il'inykh *et al.*, *J. Opt. Soc. Am. B* **10**, 1060 (1993).

Translated by Murray V. King